Supporting Information

Advanced charge utilization from $NaTaO_3$ photocatalysts by multilayer reduced graphene oxide

Tobias Meyer, Jacqueline B. Priebe, Rafael O. da Silva, Tim Peppel, Henrik Junge, Matthias Beller, Angelika Brückner, and Sebastian Wohlrab

Leibniz Institute for Catalysis at the University of Rostock, A.-Einstein-Str. 29a, 18059 Rostock, Germany

Table of contents:

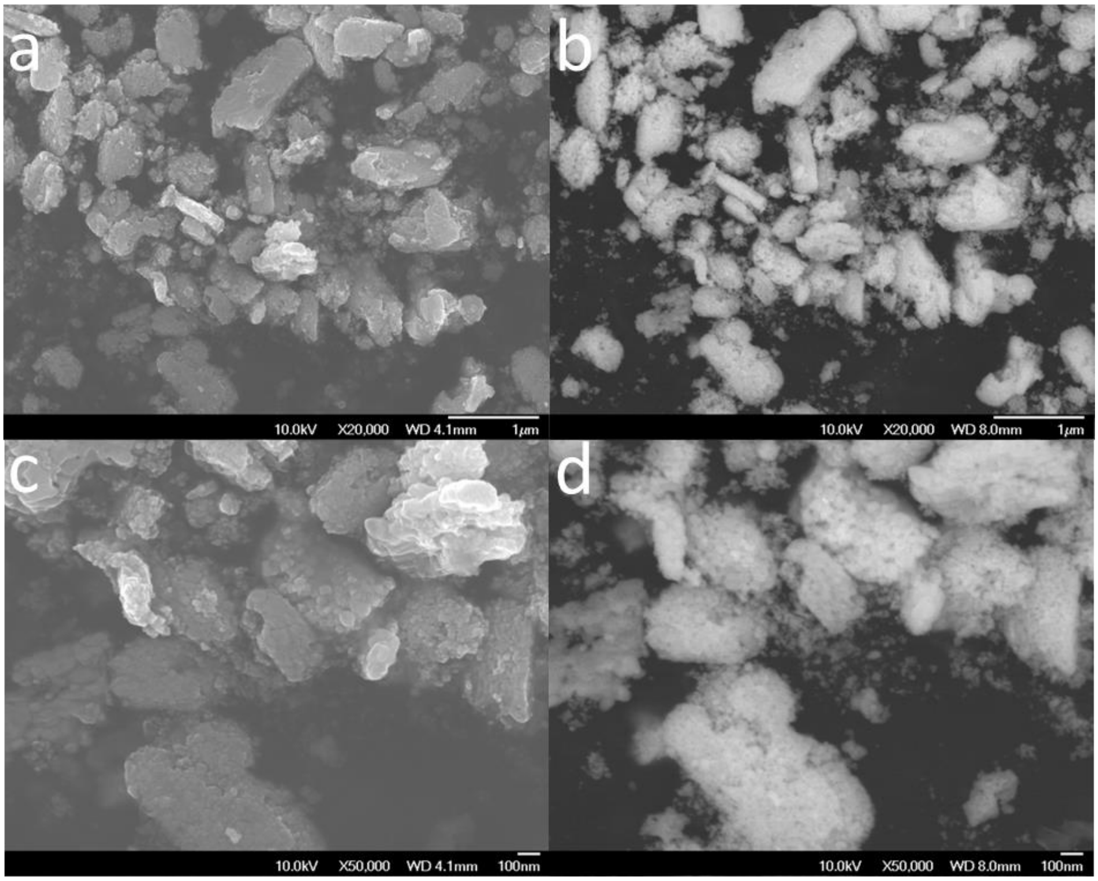

Fig. SI-1. SEM images of $NaTaO_3$ prepared by exotemplate method (EM) (a,c) topographical view with different magnifications; (b,d) COMPO mode showing the compositon contrast provided by the back scattered electrons (BSE). (d) The aggregation of the $NaTaO_3$ (EM) nanoparticles is more evident in this mode and magnification.

XPS survey spectra (Fig. SI-2) presents information on the main chemical components in the multilayer graphene oxide (m-rGO) from the measured C1s and O1s peaks which shows a significant degree of oxidation. For instance, the C 1s curve fitting can be assigned to the 4 following groups: (i) non-oxygenated C ring (C-C) at 284.5 eV, (ii) the carbon in C-O bonds (C-O) at 285.6 eV, (iii) carbonyl carbon (C=O) in the range of 287 eV and the carboxylate carbon (C-O=O) at around 289 eV. The O1s spectrum is splitted into two functional groups such as the C-O and C=O bonds respectively at 531,7 and 533,2 eV.[1,2] X-ray photoelectron spectra (XPS) were recorded by using a VG ESCALAB 220iXL.

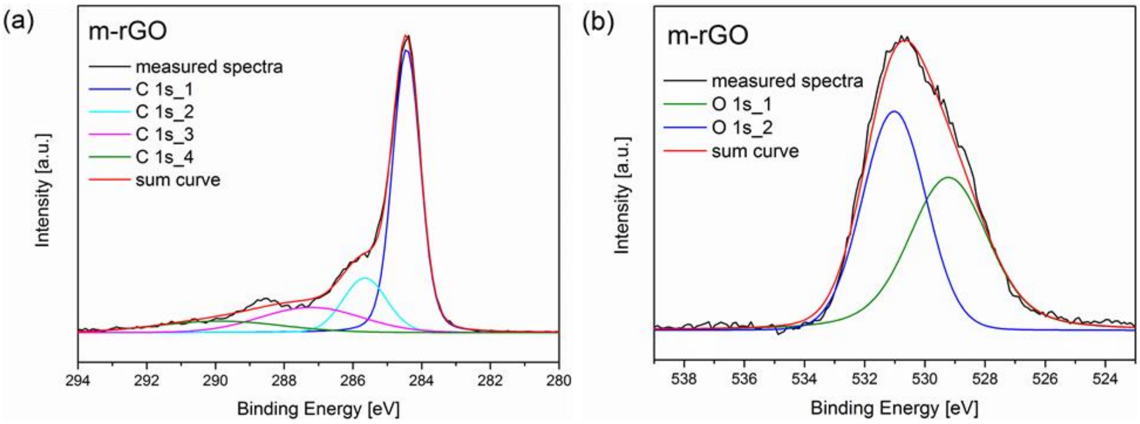

Fig. SI-2. XPS spectra of multilayer reduced graphene oxide (m-rGO): (a) C1s, (b) O1s.

Table SI-1. Amount of Carbon and Oxygen found in m-GO and m-rGO determined by Elemental Analysis and XPS. For m-GO the difference in oxygen content is not so significant than for m-rGO. Since only surface species are measured with XPS it can be derived that the reduction of the m-GO to m-rGO occurs mainly on the surface of the carbon sheets.

sample	Elemental Analysis %		XPS %	
	C	O	C	O
m-GO	54.77	43.3	64.53	35.47
m-rGO	68.4	30.1	85.16	14.84

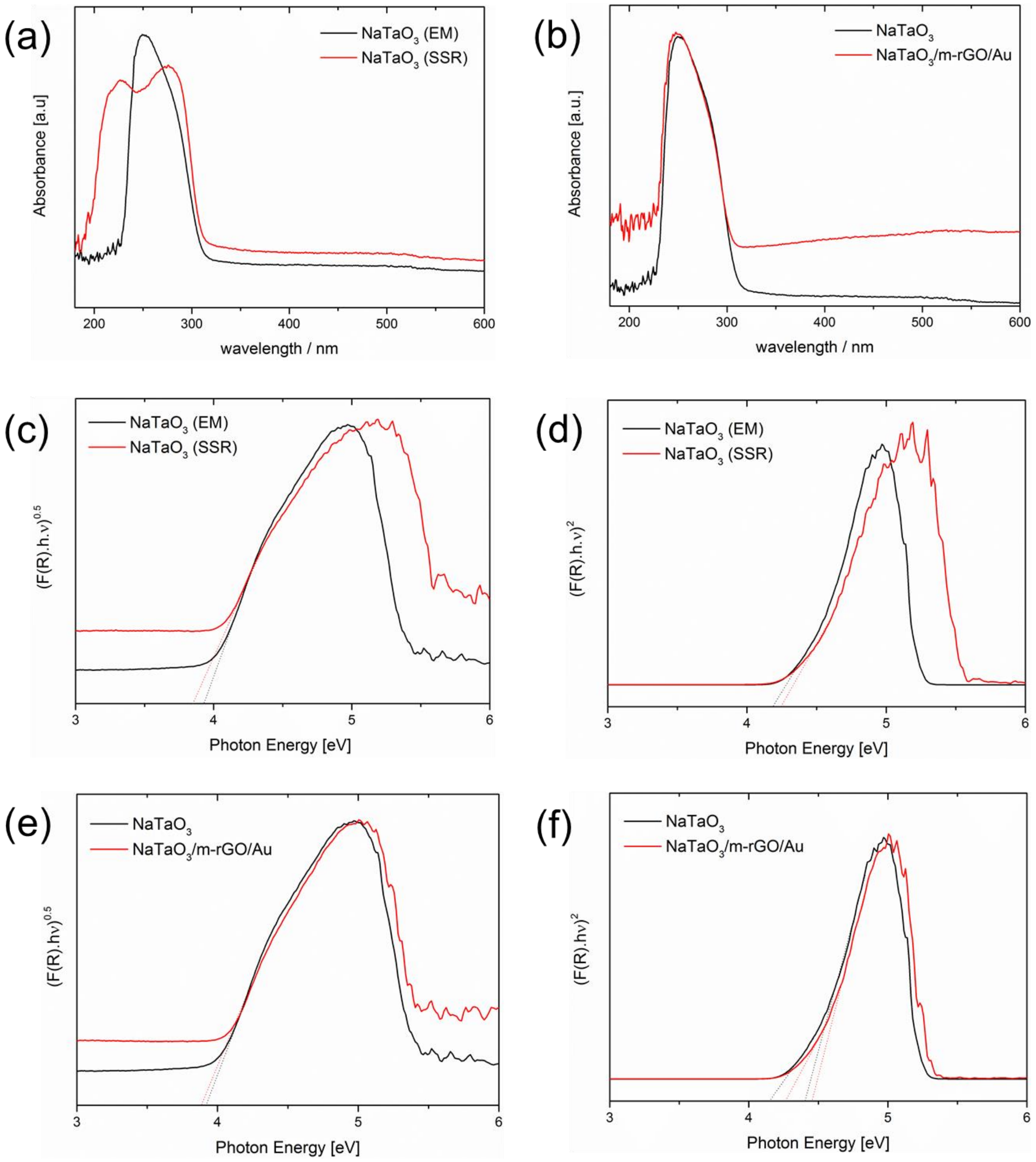

Fig. SI-3. UV-vis data of: (a) $NaTaO_3$ (EM) and (SSR); (b) $NaTaO_3$ and $NaTaO_3$/m-rGO/Au produced by the exotemplate method (EM); Tauc plot of $NaTaO_3$ (EM) and (SSR) (c) indirect band gap; (d) direct band gap; Tauc plot of $NaTaO_3$ and $NaTaO_3$/m-rGO/Au produced by EM (e) indirect band gap and (f) direct band gap. Uv-vis spectra were recorded with an AvaSpec 2048 fiber optical spectrometer.

Table SI-2. Experimental Eg values obtained from indirect and direct band gap.

Method		Band Energy (eV)	
	$NaTaO_3$ (EM)	$NaTaO_3$ (SSR)	$NaTaO_3$/m-rGO/Au (EM)
F(R) x $E^{1/2}$	3.92	3.84	3.92
F(R) x E^2	4.19	4.25	4.26-4.45

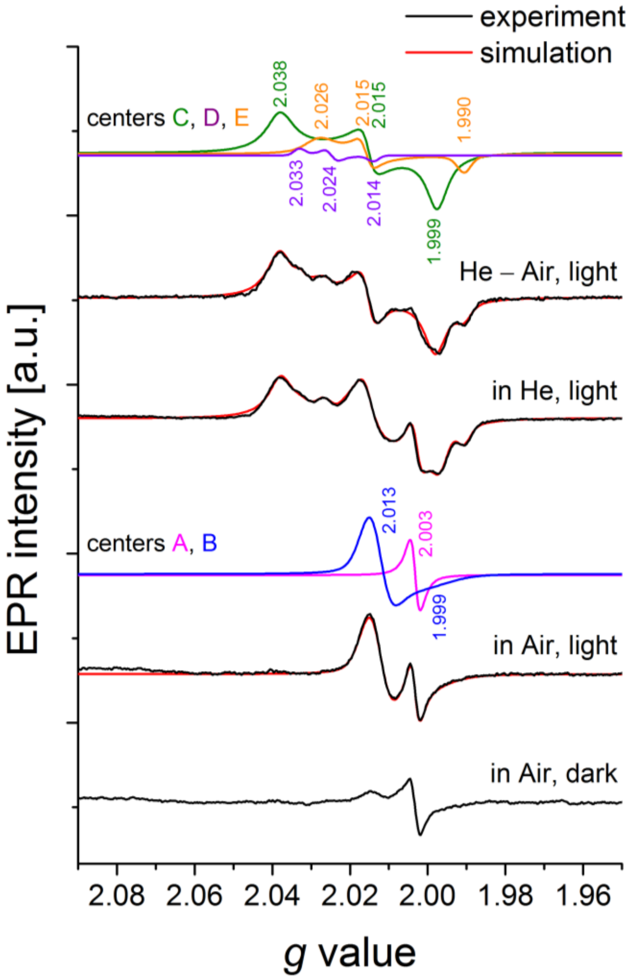

Fig. SI-4. Experimental EPR spectra of pure $NaTaO_3$ (EM) (black lines) and their simulated deconvolution (colored lines) in the dark and irradiated under ambient air as well as under helium flow. By subtracting the spectrum of the irradiated sample in air (exhibiting two bulk centres A and B) from the one under helium flow, three more surface-located centres were obtained by simulation (C, D, E).

Table SI-3. Simulation parameters corresponding to Fig. SI-1. Values in brackets are the line width in G.

center	A	B	C	D	E
Rel. Intensity	0.44	0.48	1.00	0.08	0.26
g_x	2.0029 (5.20)	2.0131 (11.3)	2.0379 (7.09)	2.0328 (5.25)	1.9915 (8.80)
g_y	-	-	2.0148 (5.33)	2.0248 (4.69)	2.0151(4.76)
g_z	-	1.9993 (18.8)	1.9971 (6.83)	2.0137 (4.28)	2.0275 (3.49)

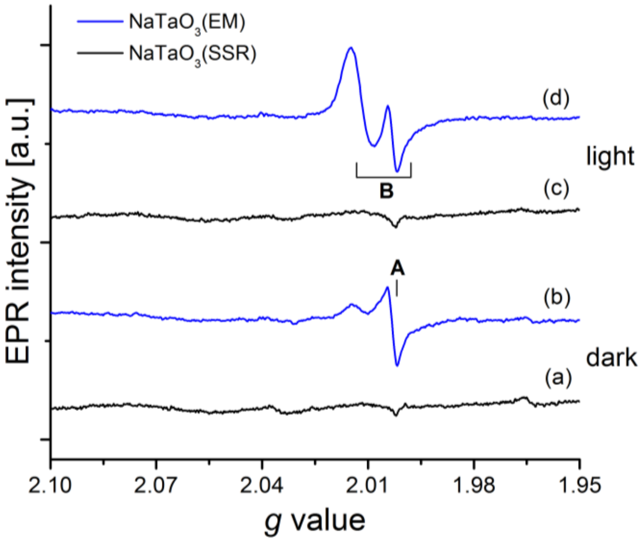

Fig. SI-5. Experimental EPR spectra of pure $NaTaO_3$ (EM) (blue) and $NaTaO_3$ (SSR) (black) in the dark (a & b) as well as UV-vis-irradiated (c & d) under ambient air. In contrast to the SSR-sample, $NaTaO_3$ (EM) exhibits a light-responding EPR signal B in presence of high amounts of oxygen.

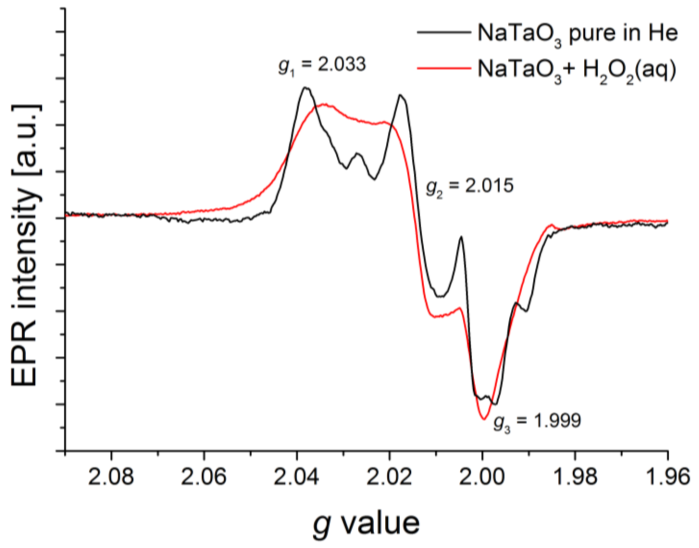

Fig. SI-6 EPR spectrum of irradiated pure NaTaO$_3$ (EM) in flowing helium at 290 K (black line) in comparison to the one of H$_2$O$_2$-treated irradiated NaTaO$_3$ (EM) recorded at 200 K (red line). Both spectra exhibit features of likely the same adsorbed paramagnetic species (O$_2^{\bullet-}$), though for the aqueous H$_2$O$_2$ sample with broadened line width and slightly shifted g_1.

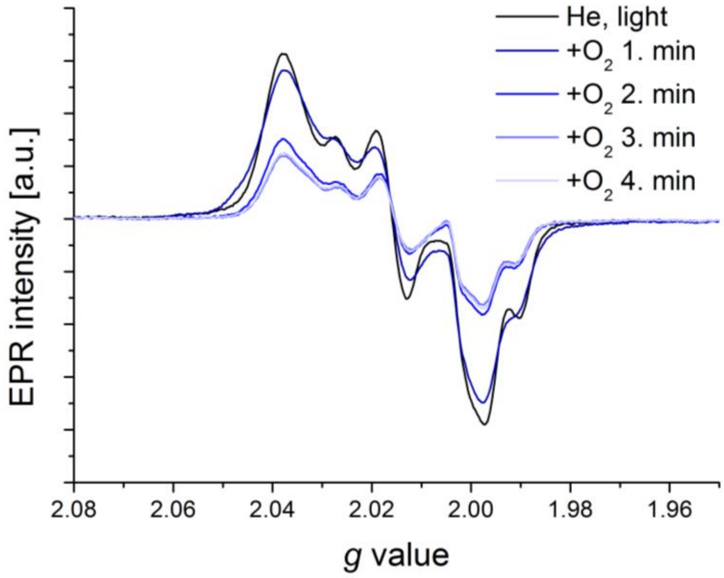

Fig. SI-7 EPR spectra of irradiated pure NaTaO$_3$ (EM) in flowing helium at 290 K (black line) with subsequent introduction of small amounts (1.5 %) of dioxygen gas (blueish lines), whereby the EPR signals get broadened due to the dipolar interaction of the adsorbed radical species to the paramagnetic gas-phase oxygen molecules.

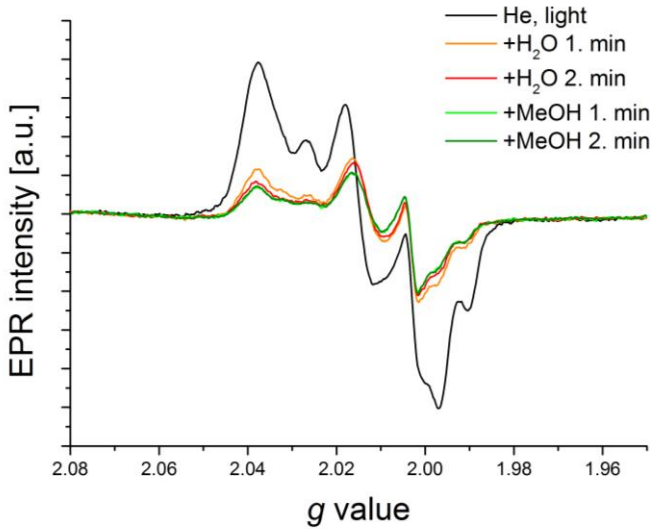

Fig. SI-8 EPR spectra of irradiated pure $NaTaO_3$ (EM) in flowing helium at 290 K (black line) with subsequent addition of water-saturated helium (reddish lines) and water/methanol-saturated helium (greenish lines). The main intensity loss of the surface-bound species was observed upon the addition of water (already after 2 minutes exposure), while a further decrease of signal B (attributed to trapped holes $O^{\bullet-}$ in the subsurface region of the catalyst) occured upon methanol introduction acting as hole scavenger.

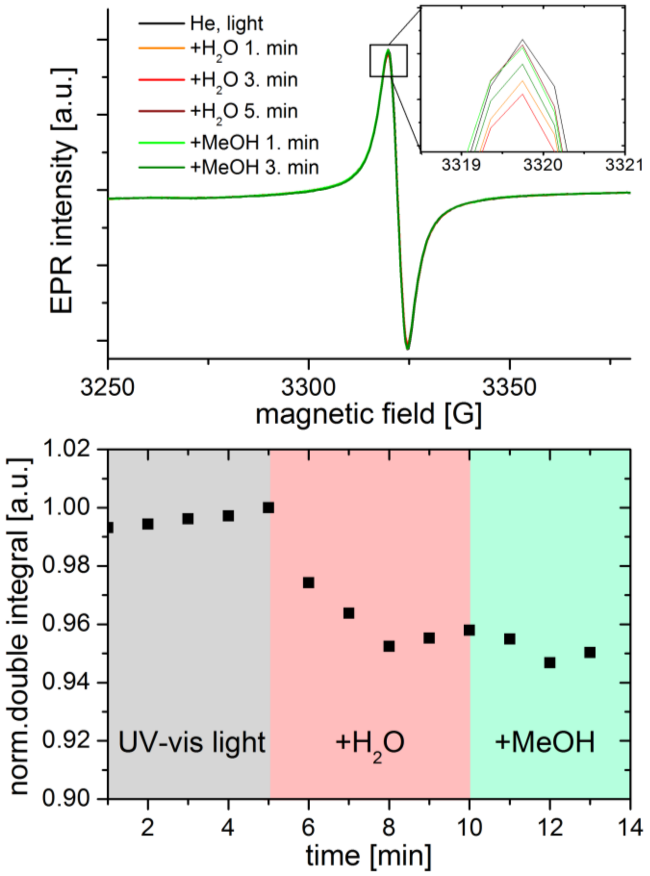

Fig. SI-9 EPR spectra (top) and corresponding normalized double integrals (bottom) of $NaTaO_3$ (EM) loaded with 0.2 wt.-% Au and 10 wt.-% m-rGO in flowing helium at 290 K with subsequent addition of water-saturated helium (reddish lines) and methanol-saturated helium (greenish lines). Upon addition of water, the signal F intensity decreases about 5 % indicating a consumption of the electrons by the protons.

References

1. Su, C. L.; Acik, M.; Takai, K.; Lu, J.; Hao, S. J.; Zheng, Y.; Wu, P. P.; Bao, Q. L.; Enoki, T.; Chabal, Y. J.; Loh, K. P., Probing the catalytic activity of porous graphene oxide and the origin of this behaviour. *Nat Commun* **2012,** *3*;

2. Jo, G.; Choe, M.; Cho, C. Y.; Kim, J. H.; Park, W.; Lee, S.; Hong, W. K.; Kim, T. W.; Park, S. J.; Hong, B. H.; Kahng, Y. H.; Lee, T., Large-scale patterned multi-layer graphene films as transparent conducting electrodes for GaN light-emitting diodes. *Nanotechnology* **2010,** *21* (17).